

Hadronization at the AdS Wall

Nick Evans¹, James French¹, Kristan Jensen² & Ed Threlfall¹

¹ *School of Physics and Astronomy, University of Southampton, Southampton, SO17 1BJ, UK*

² *Department of Physics, University of Washington, Seattle, WA98195, USA*

evans@soton.ac.uk, james.french@soton.ac.uk, kristanj@u.washington.edu, ejt@phys.soton.ac.uk

We describe hadronization events, using the AdS/CFT Correspondence, which display many of the qualitative features expected in QCD. In particular we study the motion of strings with separating end points in a back-reacted hard wall geometry. The solutions show the development of a linear QCD-like string. The end points oscillate in the absence of string breaking. We introduce string breaking by hand and evolve the new state forward in time to observe the separation of two string segments. A kink associated with this breaking evolves to the end points of the string inducing rho meson production. We explicitly compute the rho meson production at the end point.

INTRODUCTION

The AdS/CFT Correspondence [1, 2, 3, 4] provides a new tool for the study of strongly coupled gauge theories and has been extended to cover both gauge and quark [5, 6, 7, 8, 9, 10, 11, 12] degrees of freedom. Hadronization, the conversion of quark pair production into jets of hadrons, is traditionally a thorny problem in QCD. It is therefore interesting to model this process with the Correspondence.

The combination of asymptotic freedom and confinement in QCD ensures that the road from quark production to jets, as in a high-energy accelerator such as LEP, is broken up into three overlapping stages. This is the statement of factorization. For a recent review, see [13]. The first, pair production, typically occurs at high energies and so the relevant degrees of freedom are a bare quark/anti-quark pair. As they fly apart, these quarks begin to radiate soft gluons and quark/anti-quark pairs - the process known as showering - so that the relevant degrees of freedom are *dressed* quarks. Showering can be computed at high energies in QCD with effective theories including soft collinear effective theory. After the dressed quark/anti-quark pair have propagated a distance of order $1/\Lambda_{\text{QCD}}$ apart, the strong coupling and confining dynamics of QCD become relevant: the quark pair forms a highly excited colourless hadron that can and does fragment. This last conversion is known as hadronization.

The middle process of showering has been studied in different contexts via the Correspondence. A number of authors [14, 15] have computed the evolution after the injection of R charge into the $\mathcal{N} = 4$ Super Yang-Mills theory. The $\mathcal{N} = 4$ theory is strongly coupled at all scales and so there is no suppression of the emission of large transverse momentum - rather than seeing jets, the events fill the entire space surrounding the initial pair creation.

In the AdS/CFT correspondence, strings with their ends tied to a D7 brane represent a quark anti-quark pair in the dual field theory. The dual quarks have a constituent mass that goes to zero in the limit that the D7 brane fills the entire AdS space. The evolution of such pairs in the massless quark limit with separating end points was first studied in [16]. They worked in the quenched $\mathcal{N} = 2$ gauge theory obtained by placing probe D7 branes in $\text{AdS}_5 \times S^5$. Both the endpoints and the string between them fall indefinitely into the radial direction of the AdS space representing the spreading of baryon charge and energy respectively in the dual field theory as the state evolves. These states are anisotropic and their evolution naturally describes the showering of flavour. Hadron (rho meson) production can only occur on the D7 world-volume through the motion of the endpoints of the string. The production for these states was computed [16] and jet-like structures were seen.

Much attention has focused on heavy quark propagation at finite temperature [19, 20]. The $\mathcal{N} = 4$ theory is perhaps more like QCD in its non-conformal high temperature phase which is described by an AdS-Schwarzschild geometry [3]. These computations have also been inspired by attempts to reproduce jet quenching observed in heavy ion collision data at RHIC.

In this paper we wish to return to study the second and third phases of hadronization described above at zero temperature. To find a dual gravity description that behaves like QCD one must seek a non-conformal version of the AdS/CFT Correspondence that at least incorporates confinement. There has been a considerable body of work in this direction. We will work in the context of deformed AdS geometries [21, 22, 23, 24, 25, 26, 27, 28, 29] which have the benefit of being 3+1 dimensional at all energy scales and having naive perturbative dimensions for a class of operators in the UV (of course the UV is not perturbative but conformal, strongly coupled, and highly supersymmetric). Simple deformations such as

the introduction of masses for the $\mathcal{N} = 4$ matter content that break the supersymmetry to $\mathcal{N} = 2$ [22], $\mathcal{N} = 1$, [23, 24, 25] or less [26, 27, 28, 29] have been studied. These dualities are not as well understood as the original Correspondence but a number of features seem generic. In particular, the geometries dual to confining theories develop a wall structure in the interior that stops fields from penetrating to energy scales (radial distances in AdS) below the mass gap of the theory. Such a repulsive wall leads to linear potentials between quarks since they are described by the ends of a fundamental string in the geometry - typically the centre of these strings fall on to and lie close to the repulsive wall with their energy then just scaling with their length.

In fact, the imposition of a simple hard wall cut off on AdS is now frequently used to model a mass gap [30, 31, 32]. That will not be sufficient for us since we wish to evolve the strings onto the wall and therefore need the repulsion to be described by the geometry. Given that these dualities are not fully understood we will take the simplest example of a deformation with such a hard wall. So called “dilaton flow” geometries [27, 28, 29] have a non-trivial dilaton profile in a deformed AdS space. The dilaton, or on the field theory side the gauge coupling, blows up at some infra-red scale generating the wall (effectively the scale Λ_{QCD}). The wall is repulsive to strings and also to the D7 branes they are attached to, which dynamically induces both confinement [28, 33] and chiral symmetry breaking [10, 11]. Such a geometry is clearly a decent first stab at describing a QCD-like gauge theory.

Having found a model for such a theory, we follow the program of [16] and evolve strings in this geometry. In particular, we consider numerical solutions of the Polyakov string action for strings with ends tied to a D7 brane and point-like initial conditions to represent the pair creation of a quark anti-quark pair. We allow the end points to separate quickly leaving a string falling into the geometry between. It is fairly easy (though computer-time consuming) to numerically follow this evolution with pre-built numerical integrator functions such as NDSolve in Mathematica. As one might expect, in the hard wall setup the string falls onto and bounces off the wall in the radial direction - the centre of the string then oscillates, falling on to the wall repeatedly. Whilst this happens, the endpoints move apart and a longer string grows, taking up the kinetic energy near the end points. Formally, we study this process at infinite N and so there is no string breaking; instead, the string continues to evolve. Since the string can only extend so far, the endpoints eventually stop and their motion reverses. The string bounces in the three dimensional space. The model therefore correctly reproduces expectations from field theory in the large N limit.

For real QCD string breaking is presumably greatly favoured, occurring essentially as soon as there is of order Λ_{QCD} worth of potential energy in the string. In our gravity description, string breaking is captured by stringy $1/N$ effects: there will be some transition amplitude between our initial string and a final state and the actual evolution will involve a sum over all possible intermediate states, including those with two string segments. Attempts have been made to compute this breaking probability in [34, 35, 36, 37] which we do not add to here. We choose instead to study the evolution after string breaking, so we simply break our strings by hand and consider particular states with two string segments. In particular, we insert a static quark/anti-quark pair and then evolve these new *particular* strings. We simulate the inserted pair with a static string that falls straight down into the AdS space from the D7 brane. At a time of our choosing (usually once the initial string grows to a size of order $1/\Lambda_{\text{QCD}}$), we break the initial string in the middle by hand and join each half to a static segment. We then follow this broken string as it evolves.

This configuration again evolves as one might expect - the static endpoint (anti-quark) is dragged by the fast moving endpoint (quark) that it has been attached to and the endpoints (quark/anti-quark pair) of the original string are free to separate to infinity. The broken strings have a kink at the point where the static string was attached which evolves to the endpoints. The kink then causes a rapid jerk in the motion of the inserted static endpoint (anti-quark).

In the AdS/CFT Correspondence, mesons made of the quarks are associated with open strings tied to the D7 brane [9] - in fact, in the large N and strong coupling limit, rho mesons are the dominant such mode, described by a dual gauge field on the D7 world volume. The string endpoint is a source for that gauge field. The rapid jerk of an endpoint provides a mechanism for copious production of the rho mesons, in the same way that an accelerating charge radiates in classical electromagnetism. We show how to compute this production.

The rho meson and each of its radially excited states is associated with a normalizable mode in the radial direction on the D7 brane. The full production of the gauge field on the D7 world-volume can therefore be computed mode by mode. In fact the radial dynamics simply encodes the mass of the physical state and the strength with which a particular source couples to that mode. For a single mode, the calculation is just of the usual form for a moving source coupled to a massive vector field in 4d and is straightforwardly computed. A static quark (string endpoint) has a cloud of mesons around it with their density decaying with distance as an exponential of the mass. When an endpoint accelerates, it also radiates waves which correspond to the production of rho mesons

in the hadronization event. We explore this production for the rho meson and its excited states.

The solutions we present for moving string solutions provide a qualitative understanding of how hadronization may occur in QCD or related theories. We do not in this paper wish to make any claims that these computations are numerically accurate for QCD, but we hope that the mechanisms revealed will provide thought for the future modelling of hadronization in QCD. We discuss the prospects in our final section.

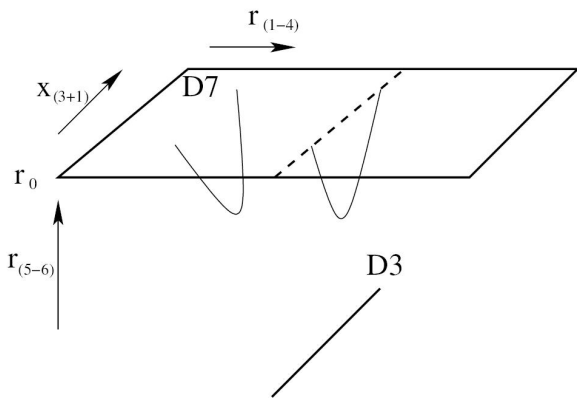


Figure 1: The basic D3-D7 system showing the coordinate labelling we use - note the D3 lies at $r = 0$. We also show two possible moving string configurations - one lies off the plane of closest approach between the D3 and the D7 and lies in a 3d space, the string with end points separating along that plane lies in just 2d. We study moving strings of the latter type.

GEOMETRIES AND QUARKS

The vacuum structure of $\mathcal{N} = 4$ $SU(N)$ super Yang-Mills gauge theory is encoded in the $AdS_5 \times S^5$ geometry

$$ds^2 = \frac{r^2}{R^2} dx_{3+1}^2 + \frac{R^2}{r^2} dr_6^2 \quad (1)$$

where $R^4 = 4\pi g_s N \alpha'^2$, g_s is the string coupling, and α' sets the string length. The dilaton is constant and there is a four form $C_{(4)} = r^4/R^4 dx^0 \wedge \dots \wedge dx^3$. Note that, in these coordinates, r (the radial direction in the six dimensional r_6 space) corresponds to the gauge theory energy scale ($r = 0$ is the infra-red). The AdS space has a boundary at $r = \infty$ and the dual gauge theory “lives” on that boundary with a metric conformal to the Minkowski space metric dx_{3+1}^2 .

To introduce a single quark flavour (really a single $\mathcal{N} = 2$ hypermultiplet), we place a D7 brane lying in the $x^0 - x^3$ and $r^1 - r^4$ directions (see Figure 1). In pure AdS, such a brane lies flat with $r_5^2 + r_6^2 = r_0^2$. The separation r_0 sets the scale of the constituent quark mass ($m_q = r_0/2\pi\alpha'$),

related to the energy of an open string with one end at the bottom of the D7 brane and the other at the AdS horizon $r = 0$. In contrast, a fundamental string with each end on the D7 brane represents a quark/anti-quark pair and the interaction energy between them. As shown in [17], for very heavy static quarks (i.e. with their ends tied to a D7 brane at $r = \infty$), the dual string hangs further and further into the bulk as the quarks are separated. The total energy of the state scales as one over the quark separation.

To provide a gravity description of a confining gauge theory, we will consider a geometry that is asymptotically AdS (the UV contains the same degrees of freedom as the $\mathcal{N} = 4$ theory) but which has a back-reacted hard wall in the IR. The simplest such example we know is a dilaton controlled deformation [27, 28]. The metric in Einstein frame for this deformed geometry is

$$ds^2 = \frac{r^2}{R^2} A^2(r) dx_{3+1}^2 + \frac{R^2}{r^2} dr_6^2, \quad (2)$$

with

$$A(r) = \left(1 - \left(\frac{r_w}{r}\right)^8\right)^{1/4}, \quad e^\phi = \left(\frac{1 + (r_w/r)^4}{1 - (r_w/r)^4}\right)^{\sqrt{3/2}}, \quad (3)$$

and the four form is as in the pure AdS solution.

Note that the dilaton (dual to the gauge coupling) and metric have a singularity at $r = r_w$ which can be loosely interpreted as the scale at which the gauge coupling diverges, Λ_{QCD} . In [38] it was argued that the best interpretation of this geometry might be as dual to the low energy theory below some UV cut off where some highly irrelevant supersymmetry breaking but $SO(6)$ preserving coupling becomes important in the $\mathcal{N} = 4$ gauge theory (a scalar mass term is an example of such an operator). For our purposes in this paper though, the geometry is simply playing the role of a back reacted hard wall to include confinement and the precise physics is unimportant.

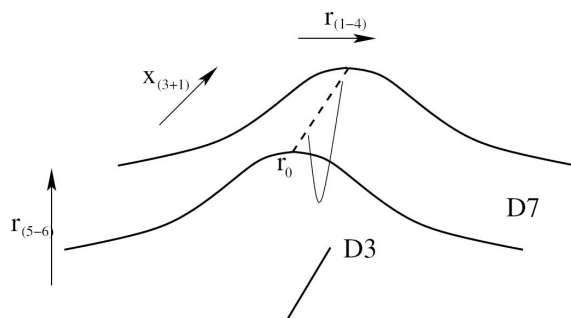


Figure 2: A sketch of a D7 embedding in the back reacted hard wall geometry for a quark with zero current mass. The bending of the D7 induces a constituent mass (non-zero minimum D3-D7 separation) for the quarks.

Quarks can generically be added to the theory by including a D7 brane as in the AdS case. The hard wall is repulsive to the D7 brane and so induces chiral symmetry breaking through the formation of a quark condensate - the details are discussed in [10, 11]. In Figure 2 we sketch the form of the D7 embedding in the geometry for the case of zero bare quark mass - the D7 is bent so that there is never a zero length string between the D3 and D7: the quarks have acquired a constituent mass.

As discussed in [28, 33] a string with ends tied to a D7 brane, corresponding to a quark pair, is repelled by the hard wall at $r = r_w$ and the string lies close to that wall - there is a linear potential between the quarks.

Conventions

Throughout this work, we consider fields living on four different spaces: the full 10d geometry, the worldvolume of a D7 brane, the worldsheet of a fundamental string, and on the Minkowski spacetime of the dual field theory. To simplify some of this chaos, we choose some conventions for how we label indices and these fields. First, we will use the upper-case latin letters (M, N, \dots) to refer to 10d spacetime indices (e.g. $G_{MN} dx^M dx^N$ is the metric on the 10d space), while lower-case latin letters (a, b, \dots) refer to worldsheet and worldvolume indices. Finally, we use lower-case Greek letters (μ, ν, \dots) to index the Minkowski directions in both the 10d geometry and D7 worldvolume (i.e. x^μ , $\mu = 0, 1, 2, 3$).

STRINGS IN PURE ADS

A study of string evolution in pure AdS was presented in [16]. Here we repeat that framework, which we will use below, and summarize the form of the results.

We work with the Polyakov action in Einstein frame

$$S_P = -\frac{1}{4\pi\alpha'} \int d^2\sigma e^{\phi/2} \sqrt{-\eta} \eta^{ab} \partial_a X^M \partial_b X^N G_{MN}, \quad (4)$$

where η_{ab} is the world sheet metric, σ^a labels the worldsheet coordinates, X^M are the embedding functions, and G_{MN} is the background metric. One is free to use the symmetries of the theory to fix the world sheet metric and we will pick the form

$$\eta_{ab} = \begin{pmatrix} -\Sigma(x, r) & 0 \\ 0 & \frac{1}{\Sigma(x, r)} \end{pmatrix}. \quad (5)$$

We pick and choose the form of the stretching function Σ problem by problem in order to keep our numerics stable.

Also, we label the timelike world sheet coordinate as τ and the spacelike as σ (i.e. $d^2\sigma = d\tau d\sigma$).

The equations of motion are

$$\begin{aligned} \partial_a [e^{\phi/2} \sqrt{-\eta} \eta^{ab} G_{MN} \partial_b X^N] \\ - \frac{1}{2} \partial_a X^P \partial_b X^N \frac{\partial}{\partial X^M} (e^{\phi/2} \sqrt{-\eta} \eta^{ab} G_{PN}) = 0. \end{aligned} \quad (6)$$

Note that the derivative in the final term acts on η^{ab} depending on the choice of Σ .

The open string boundary condition applied at the string end points $\sigma = \sigma_*$ is

$$e^{\phi/2} \sqrt{-\eta} \eta^{\sigma b} G_{MN} \partial_b X^N = 0. \quad (7)$$

However, if the string is attached to a D-brane localized at $x^M = c^M$, then this condition is replaced in the directions transverse to the brane by the Dirichlet condition $X^M = c^M$.

There are also world sheet constraints from variation with respect to η_{ab} are

$$\partial_a X^M \partial_b X^N G_{MN} = \frac{1}{2} \eta_{ab} \eta^{cd} G_{MN} \partial_c X^M \partial_d X^N, \quad (8)$$

which, with the form of η_{ab} above become

$$\dot{X} \cdot X' = 0, \quad (9)$$

$$\dot{X}^2 + \Sigma^2 X'^2 = 0, \quad (10)$$

where \dot{X} indicates $\partial_\tau X$ and X' denotes $\partial_\sigma X$.

We will also need to compute the energy of the strings that we generate. That energy can be determined from the 10d space-time stress energy tensor

$$\begin{aligned} T^{MN} &= -\frac{2}{\sqrt{-G}} \frac{\delta S_P}{\delta G_{MN}(x)} \\ &= \frac{1}{2\pi\alpha'} \int d^2\sigma e^{\phi/2} \sqrt{-\eta} \eta^{ab} \partial_a X^M \partial_b X^N \frac{\delta^{10}(x-X)}{\sqrt{-G}}. \end{aligned} \quad (11)$$

The conserved energy is then given by the integral over the 9d space of T_0^0 ,

$$E = \frac{1}{2\pi\alpha'} \int d^2\sigma e^{\phi/2} \sqrt{-\eta} \eta^{ab} \partial_a X^0 \partial_b X_0 \delta(t - X^0). \quad (12)$$

If we rewrite the delta function as

$$\delta(t - X^0) = \frac{\delta(\tau - \tau_*(\sigma))}{|\partial_\tau X^0(\tau_*(\sigma), \sigma)|}, \quad (13)$$

where $\tau_*(\sigma)$ is the solution to $X^0(\tau_*(\sigma), \sigma) = t$, we can then integrate over τ to find

$$E = \frac{1}{2\pi\alpha'} \int d\sigma e^{\phi/2} \sqrt{-\eta} \frac{\eta^{ab} \partial_a X^0 \partial_b X_0}{|\partial_\tau X^0|} \Big|_{\tau=\tau_*(\sigma)}. \quad (14)$$

Separating Quark Solutions

In [16] falling strings in AdS with endpoints separating in the Minkowski directions x^μ were studied - those solutions describe states with massless quarks in the basic $\mathcal{N} = 2$ theory described by the D3-D7 system. For massless quarks, the D3 lies within the D7 and the strings with ends on the D7 are free to come arbitrarily close to the D3s at $r = 0$. The solutions they found had the endpoints separating in x and, at late times, falling in r along geodesics. The centre of the string fell faster in r leaving a curved string between the endpoints. They showed that kinks in the initial condition of the string were quickly smoothed out by the inflation-like growth of the string.

We now wish to begin to make contact to QCD where, although the current quark masses are small (for the light quarks), they nevertheless obtain a large constituent mass from the chiral symmetry breaking dynamics of the theory. For this reason, we will work with the D3-D7 system in a configuration where the D3 and D7 do not coincide (i.e. the dual quarks are massive). Later, we will consider the setup where we embed the D7 in the deformed AdS of Eq. (2).

As shown in Figure 1, the motion of a string ending on the D7 is generically a three dimensional problem. The string can move in the Minkowski directions x^μ and the r^{1-4} directions on the D7 whilst the centre of the string may droop into the remaining two r^{5-6} directions of the geometry. For simplicity, we will restrict the motion to two dimensions - that is, we will look at strings lying at the point of closest approach between the D3 and the D7, with ends separating in the x^μ directions. There is no hard computational block to performing the more generic computation, but we believe we can pick out the crucial physics within the simplified set-up.

So that our analysis can be compared to that in [16], we will follow their example and define an inverse radial coordinate

$$z^2 = \frac{R^4}{r_5^2 + r_6^2}. \quad (15)$$

The D7 brane embeddings are more complicated in these coordinates, but we will only work with strings at the point of closest approach to the D3, z_0 . The strings we study therefore lie at $r_1^2 + r_2^2 + r_3^2 + r_4^2 = 0$. The constituent mass of the quarks is then $m_q = \frac{R^2}{2\pi\alpha'z_0}$. The AdS boundary is now located at $z = 0$ and the IR (or the D3 branes) is at $z = \infty$. The string then falls in the 3d space parameterized by the Minkowski directions $x^0 \equiv t, x^1 \equiv x$ and radial coordinate z with metric

$$ds^2 = \frac{R^2}{z^2} (-(dx^0)^2 + (dx^1)^2 + dz^2). \quad (16)$$

The general initial conditions for such a string are parameterized by specifying the embedding functions t, x , and z and their derivatives at world sheet time $\tau = 0$ as a function of σ . As an example, consider the initial condition

$$t(\sigma, 0) = 0, \quad x(\sigma, 0) = 0, \quad z(\sigma, 0) = z_0. \quad (17)$$

Note that this initial condition corresponds to a configuration where the string is initially contracted to a point. Since $X'(\sigma, 0) = 0$, the first world sheet constraint Eq. (9) is satisfied and the second Eq. (10) is simply $\dot{X}^2 = 0$.

Of course, the point-like initial conditions Eq. (17) are not sufficient to specify the subsequent string evolution. We must also specify the τ -derivatives at $\tau = 0$ consistent with the constraint equations Eq. (8). Consistent point-like initial conditions are then specified by two free functions, $\dot{x}(\sigma, 0)$ and $\dot{z}(\sigma, 0)$. The last derivative, $\dot{t}(\sigma, 0)$, is fixed by the constraints to be

$$\dot{t}(\sigma, 0) = \sqrt{\dot{x}(\sigma, 0)^2 + \dot{z}(\sigma, 0)^2}. \quad (18)$$

As an example, we consider strings with initial derivatives

$$\dot{z}(\sigma, 0) = Cz_0 \sin \sigma, \quad \dot{x}(\sigma, 0) = Dz_0 \cos \sigma, \quad (19)$$

where the string endpoints are located at $\sigma_* = 0, \pi$. This set of initial conditions has two free parameters C and D that essentially set the string's momentum in the z and x directions respectively (the total string's x momentum obviously vanishes - D sets the size of the momentum in the x direction of either half of the string). Strings generated from large D and small C will have end points that quickly separate in the x direction, so that the dual field theory state contains a back-to-back quark/anti-quark pair with large momenta.

The string generated from these initial conditions has some energy. Using Eq. (14), and the initial value of $\dot{t}(\sigma, 0)$,

$$\dot{t}(\sigma, 0) = z_0 \sqrt{C^2 \sin^2 \sigma + D^2 \cos^2 \sigma}, \quad (20)$$

we find that the total energy of this string is

$$\begin{aligned} E &= \frac{1}{2\pi\alpha'} \int d\sigma g_{00} \frac{\partial_r X^0}{\Sigma} \Big|_{\tau=0} \\ &= \frac{R^2}{2\pi\alpha'z_0} \int d\sigma \sqrt{C^2 \sin^2 \sigma + D^2 \cos^2 \sigma}, \end{aligned} \quad (21)$$

where we have normalised the stretching function Σ by $\Sigma(z_0) = 1$. The constant C lets us choose the initial speed of the centre of the string in the z direction whilst D (in the large D/C limit) picks the total energy of the string.

With these initial conditions we can solve the three equations of motion (6) provided we also impose the end point

boundary conditions

$$t'(\sigma_*, \tau) = 0, \quad x'(\sigma_*, \tau) = 0, \quad z(\sigma_*, \tau) = z_0. \quad (22)$$

Note that our choices of initial time derivatives above are also consistent with these boundary conditions. Finally, since the initial conditions satisfy the constraint equations Eq. (8), the evolved string satisfies them at all times.

A judicious choice of the stretching function allows ND-Solve in Mathematica to follow the evolution for a considerable time. Here we pick

$$\Sigma = z_0^2/z^2 \quad (23)$$

To check the consistency of the solutions along the time evolution we monitor the total energy of the configuration using Eq. (14) - for all our solutions energy is conserved at, at least, better than the 1% level through the evolution. For the simple solutions in AdS the conservation is much better than 1%.

In Figure 3 we show the evolution of such a configuration with C and $D = 1$ and $z_0 = 0.5R$. As the end points separate, the string droops down into the bulk of AdS . Increasing C only serves to push the middle of the string down into AdS faster. Overall, this picture is consistent with the usual expectations from static strings in AdS and with the results described at zero mass in [16]. In particular, the fact that the string can penetrate indefinitely into the bulk of AdS reflects the conformal $1/r$ potential between two quarks. Of course, this behaviour is closer to the asymptotically free regime of QCD than the confining phase. We now turn to modelling the latter.

STRINGS WITH A HARD WALL

We will now study the motion of strings in the deformed-AdS geometry Eq. (2) to represent quark/anti-quark pair production in a confining gauge theory. As for the strings we studied in the last section, we will again set the string in motion in the x direction whilst localised in the r^{1-4} directions at the point of closest approach of the D7 to the D3 brane - see Figure 2. The embedding function of the D7 brane will not therefore play any role in the computation other than determining that closest approach point, z_0 . In practice, even z_0 would be a phenomenological parameter that would need to be fitted to the current quark mass - for the qualitative analysis here we set $z_w/z_0 = 2$ but the precise value is not important (if one made the ratio very large then the quarks would become heavy relative to the scale $\Lambda_{QCD} \sim 1/z_w$ representing a large bare and constituent quark mass).

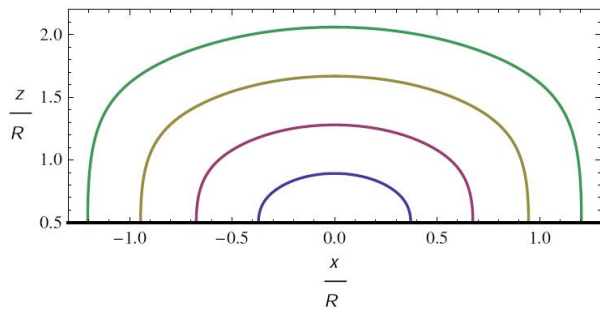
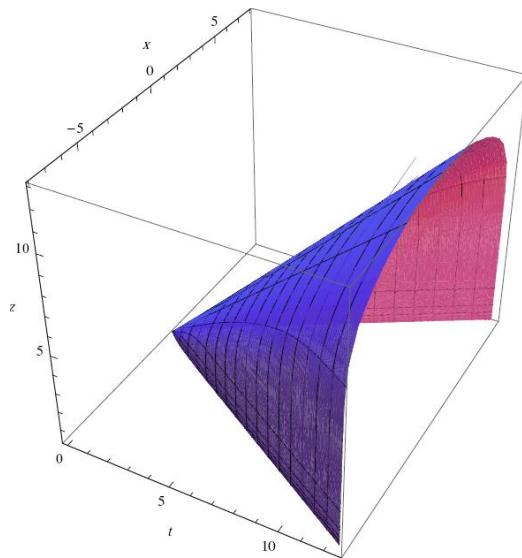


Figure 3: The evolution of a string with end points on a D7 brane at $z_0 = 0.5R$ in pure AdS with the initial conditions Eq. (17,19) and parameters $C = D = 1$. The top plot shows the string worldsheet evolution and the bottom a series constant time slice shots of the strings motion at $t = 0.4R, 0.8R, 1.2R$, and $1.6R$.

We can now consider the evolution of strings in this geometry using initial conditions like those we used above in pure AdS - that is, we look at a point-like string with separating end points. For simplicity, we will take almost exactly the same initial conditions. We maintain the conditions in Eqs. (17),(19) but to satisfy the constraint Eq. (10) with the new metric, we need a new initial condition for $\dot{t}(\sigma, 0)$:

$$\dot{t}(\sigma, 0) = z_0 \sqrt{(C^2/A^2(z_0)) \sin^2 \sigma + D^2 \cos^2 \sigma}. \quad (24)$$

Since $A(z)$ rapidly becomes unity away from the wall $z = z_w$, these strings are generated from essentially the same initial conditions as in the pure AdS analysis. We use the same stretching function Σ as in the AdS case here, Eq. (23). We plot the resulting string evolution in Figure 4.

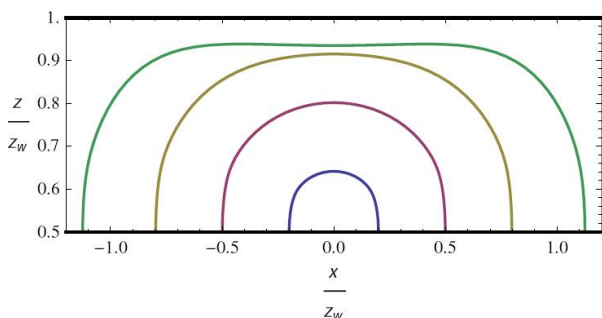
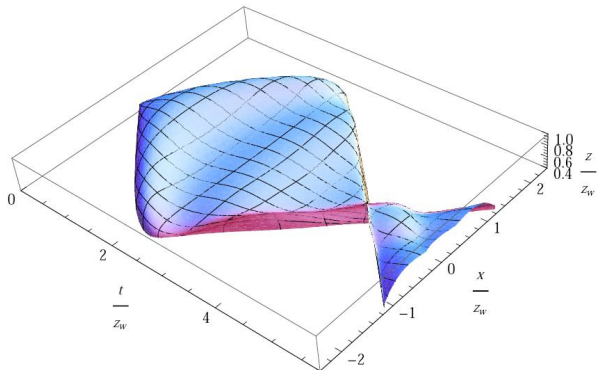


Figure 4: String evolution in a hard wall geometry. Here we set $C = 2.5$, $D = 0.5$ in the initial conditions Eqs. (17,19), and choose $z_0 = 0.5z_w$ to set the quark mass. The top plot shows the world sheet evolution. The bottom plot shows time slices through the world sheet at times $t = 0.2z_w, 0.5z_w, 0.8z_w$, and $1.1z_w$.

The solution plotted in Figure 4 shows many of the properties one would expect. In particular, as the centre of the string approaches the hard wall, it is repelled and a straight section of string builds against the wall - this is the formation of the naive QCD string. We are working at infinite N where string breaking is forbidden and so, rather than breaking, the string continues to evolve. The centre of the string begins to bounce off the hard wall and starts oscillating between the position of the D7 brane and the hard wall. Meanwhile, as the potential energy in the string grows and the quarks separate, the quarks' kinetic energy begins to be sucked into the string - they slow. Eventually the quarks are brought to a halt and the string between them begins to contract, reversing the quarks' motion until they pass through each other. This oscillation will continue indefinitely in the absence of string breaking.

We conclude that the inclusion of a hard wall does indeed begin to move the description of quark pair production closer to the expected behaviour in QCD. In the next section we will discuss how to include string breaking and thereby allow two separated jets to emerge.

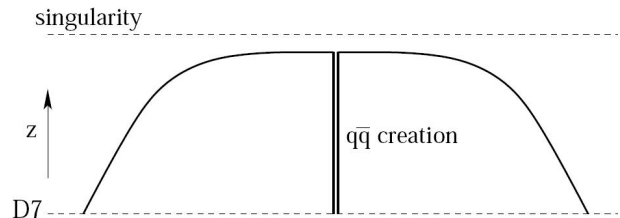


Figure 5: Sketch of the insertion of a quark anti-quark pair into the string evolution to represent string breaking.

STRING BREAKING

Our analysis of hadronization so far lacks one crucial ingredient with respect to QCD - there is no string breaking and therefore no hadronization! String breaking is an inherently $1/N$ effect and so absent from the AdS/CFT Correspondence in the tractable limit we study. Some progress has been made in studying this process though - if the string lies within the D7 worldvolume where it can break directly the rate is computable [34, 35, 36, 37] and is of order $1/N$. When the string lies away from the D7 there must be a quantum fluctuation that brings the string back to the D7 where it can break - estimates for this process can be found in [36, 37]. Here we do not wish to add to these computations. Our instinct instead is to assume that in QCD the string will break with essentially probability one as soon as there is of order Λ_{QCD} of potential energy stored in the string. We can model this on the gravity side by breaking our string at the corresponding time.

We can insert a quark/anti-quark pair into the evolution of our strings by hand. An unpaired quark corresponds to a string stretched from the D7 brane to the D3 branes. A static solution of this form with a new choice of stretching function ($\Sigma = A(z)/A(z_0)$) is

$$t(\tau, \sigma) = \frac{2(z_0 - z_s)\tau}{\pi A(z_0)} \quad (25)$$

$$z(\tau, \sigma) = \frac{2}{\pi} (z_0 - z_s)\sigma + 2z_s - z_0,$$

where x is constant. This solution satisfies the equations of motion, the constraint equations and the boundary conditions for all τ and σ . It is a straight string stretching from z_0 (at $\sigma = \pi$) through the point z_s (at $\sigma = \pi/2$).

We can therefore split our string in the centre and complete it to the D7 brane with a straight string segment as shown in Figure 5. As an example we will split the string solution shown in Figure 4 at the point where the centre of the string starts to bounce off the wall ($t = 1.13z_w$) - the QCD string has roughly just formed at this point in the time evolution. At the splitting time t_s (τ_s in world sheet time) when $t(\tau_s, \pi/2) = t_s$ and $z(\tau_s, \pi/2) = z_s$ we use the new initial conditions for the range $\pi/2 < \sigma \leq \pi$.

Strictly inserting the extra string length does not conserve energy for the half string piece - our solutions below do have sufficient initial energy that the straight string is slightly less than a 10% correction to the total energy. We don't expect the non-conservation to have any great effect on the qualitative behaviour of the solutions we display. In fact since we only study the evolution of one half of the initial string configuration one could imagine that some asymmetry in the distribution of energy between the two halves might be induced in the string breaking in any case. One could also splice out a straight string section in the middle of the initial string before inserting the vertical string pieces back to the D7 brane but we again would expect to see little qualitative change in the behaviour of the solutions.

The time evolution of the half string segment can now be followed and we show such a numerical solution in Figure 6. The solution again behaves in accordance with naive expectations - the fast moving end point of the string continues to move, whilst two kinks in the string induced by the breaking propagate to the end points. When the kink arrives at the static end point, it is jerked (along with the entire string segment) in the direction of motion of the fast end point. Similar evolution of broken strings may be found in [39]. Following the evolution without further string breaking leads to oscillations of the end points in the segment's centre of mass frame, which separates infinitely far away from the other broken string segment. We also plot in Figure 7 the motion of the two end points of the string through this evolution - the string end points are special because they source a gauge field on the D7 brane world volume which corresponds to rho meson production. We will compute this production in the next section.

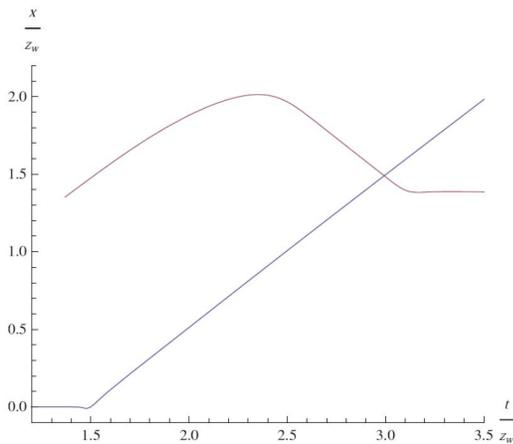


Figure 7: Plot of the string end point motion for the

configuration in Figure 6.

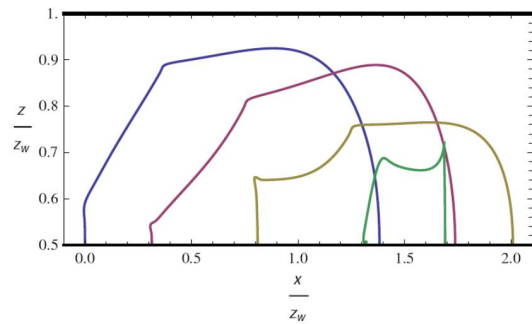
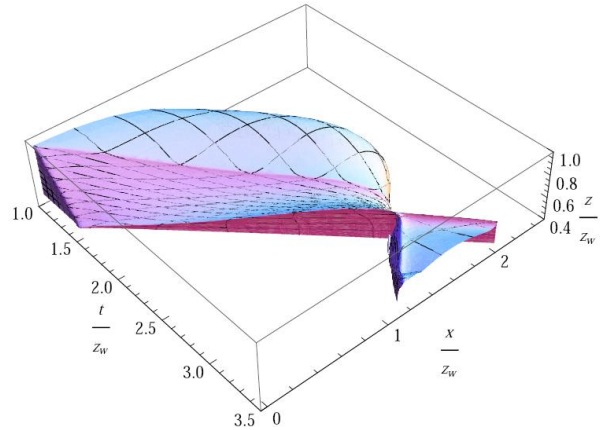


Figure 6: We show a string world sheet evolution after imposing string breaking. The initial condition involves half of the string from Figure 4 at time $t = 1.13z_w$ broken and extended by a straight string back to the D7 brane at $\sigma = \pi/2$ to $\sigma = \pi$. The top plot is again the world sheet evolution and the bottom plot slices taken at $t = 1.4z_w, 1.8z_w, 2.3z_w,$ and $3.2z_w$

RHO MESON PRODUCTION

To understand how the string solutions above radiate energy into hadronic modes, one must study the electromagnetic theory on the surface of the D7 brane. For simplicity, we will assume that the D7 of Figure 2 has been pushed out sufficiently far away from the hard wall in the geometry Eq. (2) that we may treat the 10d geometry as AdS. Further, we assume that the D7 is essentially flat. That is, we will approximate the D7 embedding with the flat embedding of a D7 in pure AdS down to $r = r_0$ with induced metric

$$P[G] \equiv g = \frac{\rho^2 + r_0^2}{R^2} dx_4^2 + \frac{R^2}{\rho^2 + r_0^2} (d\rho^2 + \rho^2 d\Omega_3^2). \quad (26)$$

Here, ρ is the radial direction on the world volume of the D7 so that $\rho^2 = r_1^2 + r_2^2 + r_3^2 + r_4^2$. Although these approximations may seem a little crude we will see that the ρ dependence of the problem enters essentially just through the mass of the mesonic states which can therefore be easily altered to any more complicated set up.

The end points of the string act as electrically charged sources for the gauge field that lives on the world volume of the D7 brane. The equation of motion for that gauge field follows from the variation of the electromagnetic action on the brane,

$$S_{\text{EM}} = -\frac{1}{4} \int d^8x \sqrt{-g} F_{ab} F^{ab} + \int d^8x \sqrt{-g} j^a A_a. \quad (27)$$

The variation of the gauge field gives both the equation of motion and the boundary action,

$$\delta S_{\text{EM}} = \int d^8x \sqrt{-g} \delta A_b \left[\frac{1}{\sqrt{-g}} \partial_a (\sqrt{-g} F^{ab}) + j^b \right] + \delta S_{\text{bdy}}, \quad (28)$$

so that the equations of motion are just Maxwell's equations,

$$\frac{1}{\sqrt{-g}} \partial_a (\sqrt{-g} F^{ba}) = j^b, \quad (29)$$

and there is a boundary action (at $\rho = 1/\epsilon \rightarrow \infty$)

$$\delta S_{\text{bdy}} = - \int_{\rho=1/\epsilon} d^4x d\Omega_3 \sqrt{-g} \delta A_a F^{\rho a}. \quad (30)$$

Let us first understand the solutions in the absence of a source.

Rho mesons

The propagating modes of the gauge field arrange themselves into multiplets of the $SO(4)$ isometry group of the S^3 . The resulting Kaluza-Klein fields each map to different operators of the gauge theory; in particular, the singlet on the S^3 maps to a conserved baryon current [9]. To study this current, we therefore give the solutions of Eq. (29) without sources for the modes that only have non-zero A_μ and are singlets on the S^3 . We impose the gauge choice $\nabla_\mu A^\mu = 0$. The equation of motion in the absence of sources is then [9]

$$\mathcal{D}A_\mu = -\frac{1}{\rho^3} \partial_\rho (\rho^3 \partial_\rho A_\mu) - \frac{R^4}{(\rho^2 + r_0^2)^2} \nabla_{(4)}^2 A_\mu = 0, \quad (31)$$

where $\nabla_{(4)}^2 = \eta^{\mu\nu} \partial_\mu \partial_\nu$ is the scalar Laplacian in Minkowski space and \mathcal{D} is a second-order differential operator. Fourier transforming in the Minkowski directions, we can write the equation above as an eigenvalue equation in the radial coordinate with eigenfunctions $f_n(\rho)$ given by

$$f_n(\rho) = I_n \frac{{}_2F_1(-n, -n-1, 2; -\rho^2/r_0^2)}{(\rho^2 + r_0^2)^{n+1}}, \quad (32)$$

where the I_n are normalization constants, $n = 0, 1, 2, \dots$, and eigenvalues

$$M_n^2 = 4(n+1)(n+2) \frac{r_0^2}{R^4} \quad (33)$$

The solutions to Eq. (31) are therefore given by the modes $A_{\mu,n} = \epsilon_\mu f_n(\rho) e^{ik_n \cdot x}$ with $k_n^2 = -M_n^2$.

These states have a discrete mass spectrum and are identified with the rho mesons of the dual gauge theory. The factor of $r_0^2/R^4 \sim m_q^2/\lambda$ indicates that the meson masses are much smaller than the quark mass at large 't Hooft coupling. Moreover, the f_n (with appropriate choices of the I_n normalizations) are orthonormal functions (subject to the weight factor w)

$$\int d\rho w f_n f_m = \delta_{mn}, \quad w = \frac{\rho^3 R^4}{(\rho^2 + r_0^2)^2}. \quad (34)$$

The corresponding choice of normalization is given by

$$I_n^2 = 2(n+1)(n+2)(3+2n). \quad (35)$$

We are using the solutions appropriate for the $\mathcal{N} = 2$ D3-D7 configuration here rather than those for a bent brane as in Figure 2. However, as we will see, the holographic directions only enter into our final radiation computation through the masses they endow the four dimensional rho mesons and the value of I_n , the normalization of the wave functions. In the more complicated case, one could simply switch the spectrum and normalizations as appropriate.

Green's Functions

To observe the emission of rho mesons by the string end points we will solve (29) by means of a Green's function for the field A_μ . For the minimum-energy configuration quark (a string connecting the D3 and D7 at their point of closest approach) the endpoint lies at $\rho = 0$ where the volume of the three-sphere is zero and hence the Green's function is a constant on the three-sphere (the equivalent of the f_n functions for R-charged states fall to zero at $\rho = 0$). This implies that there is no production of R-charged rho mesons associated with non-trivial spherical harmonics on the S^3 . For a more generic string motion such states would be produced. Moreover, since the sources do not move in the r^{1-4} four-plane, both the radial and angular components of the source current j^a vanish and thus A_ρ and A_i (the components of the gauge field along the S^3) also vanish in this gauge. We can therefore consider only the Minkowski components of the Green's function.

Having chosen the Lorentz gauge, that Green's function satisfies

$$\mathcal{D}G_\mu^{\mu'} = \frac{1}{\rho^3} \delta_\mu^{\mu'} \delta(\rho - \rho') \delta(x^\nu - x^{\nu'}), \quad (36)$$

where \mathcal{D} is the differential operator defined in Eq. (31). Since the equation of motion for the gauge field in the presence of our source is given by

$$\mathcal{D}A_\mu = \eta_{\mu\nu} j^\nu, \quad (37)$$

the full solution for an arbitrary current distribution j^μ follows from the convolution integral

$$A_\mu(x) = \int d^8 x' \sqrt{-g} G_\mu^{\mu'}(x, x') \eta_{\mu'\nu'} j^{\nu'}(x'). \quad (38)$$

The actual current distribution will be localized on the worldline of the string endpoint and will take the form $j^\mu = q \dot{x}^\mu \delta^8(x)$ where the dot represents differentiation with respect to proper time.

In order to obtain the Green's function, let us expand in the basis of eigenfunctions describing the rho mesons used in Eq. (32) so that $G_\mu^{\mu'}(\rho, x^\nu; \rho', x^{\nu'}) = \sum_n f_n(\rho) f_n(\rho') \bar{G}_{n,\mu}^{\mu'}(x^\nu, x^{\nu'})$. Inserting this form into Eq.(36), multiplying by $\rho^3 f_m$ and integrating over all space we find that the four-dimensional functions \bar{G}_n are just the Green's functions for massive vectors in Minkowski spacetime with masses corresponding to the rho meson masses.

Boundary Data

The near-boundary behaviour of the gauge field is related to the one-point function of the dual conserved baryon current in the field theory. In particular, that one-point function is given as

$$\langle J^\mu(x^\nu) \rangle = \lim_{\epsilon \rightarrow 0} \frac{\delta S_{\text{SUGRA}}}{\delta A_\mu(x^\nu, 1/\epsilon)}, \quad (39)$$

where S_{SUGRA} is the on-shell bulk gravity action and the bulk gauge field A_μ is the singlet mode on the S^3 . Using the variation of the bulk action in Eq. (28), the boundary current is simply

$$\langle J^\mu(x^\nu) \rangle = - \lim_{\epsilon \rightarrow 0} \rho^3 \eta^{\mu\nu} \partial_\rho A_\nu(x^\nu, \rho)|_{\rho=1/\epsilon}. \quad (40)$$

We can therefore write a bulk-to-boundary Green's function that relates the bulk source to the boundary current. In particular, we write

$$\langle J^\mu(x^\nu) \rangle = \int d^8 x' \sqrt{-g} \mathcal{G}_{\mu'}^\mu(x^\nu; x') j^{\mu'}(x'), \quad (41)$$

where we define the bulk-to-boundary Green's function \mathcal{G} as

$$\mathcal{G}_{\mu'}^\mu(x^\nu; x^{\nu'}, \rho') \equiv \sum_n 2(-1)^n I_n f_n(\rho') \bar{G}_{n,\mu'}^\mu(x^\nu, x^{\nu'}), \quad (42)$$

where the f_n are the eigenfunctions in Eq. (32) and \bar{G}_n is the 4d Green's function for a massive vector as before. The factor of $2(-1)^n I_n$ comes from the insertion of the near-boundary expansion of the f_n 's,

$$f_n(\rho) = (-1)^{(n+1)} I_n \frac{1}{\rho^2} + O(\rho)^{-3}, \quad (43)$$

into the form of the boundary current in Eq. (40).

Retarded Potential

We have now reduced the problem to solving for each mode G_n the retarded potential for a massive field in flat space. The retarded potential takes the form [40]

$$\bar{G}_{\mu'}^\mu = \frac{1}{4\pi} \theta(t - t') (\delta(\sigma) + V(\sigma) \theta(-\sigma)) \delta_{\mu'}^\mu. \quad (44)$$

Here we use the Synge world-function $\sigma = \frac{1}{2} \eta_{\mu\nu} (x - x')^\mu (x - x')^\nu$. The non-singular part of the solution is given by $V(\sigma) = -\frac{M_n}{\sqrt{-2\sigma}} J_1(M_n \sqrt{-2\sigma})$ where J_1 is the Bessel function of order 1.

Static String End Point

As a first example of using this formalism we will compute the baryon density around a static quark. Consider such a charge at $x = 0$ and at $\rho = 0$ ($r = r_0$), the point of closest approach on the D7 brane. We will concentrate on the temporal component of the gauge field A^0 which is dual to the operator $\bar{\psi}\gamma^0\psi$, the quark density.

One seeks to evaluate the integral over the past trajectory of a point source moving with a constant speed in a ‘static gauge’ given by $x' = \beta t'$. Doing the spatial integral using the fact that the source is located at a point in the space-like dimensions leaves one with the integral

$$\langle J^0(x^\nu) \rangle_n = \frac{2(-1)^n I_n^2 q}{4\pi} \times \int dt' \theta(t - t') (\delta(\sigma) + V(\sigma)\theta(-\sigma)) \frac{d\tau}{dt'} \cdot \frac{dt'}{dt} \quad (45)$$

where we have used the fact that $f_n(\rho = 0) = I_n$.

The time component of the four-velocity is actually cancelled by a Lorentz factor coming from the splitting of Minkowski spacetime into space-like sections when integrating along the particle worldline. The two contributions to the integral are easily computed (for the non-singular piece due to the massive field using the integration variable $u \equiv M_n \sqrt{-2\sigma}$) giving the correctly Lorentz-covariant expression (the γ is the usual boost factor)

$$\langle J^0(x^\nu) \rangle_n = \frac{2(-1)^n I_n^2 q \gamma e^{-M_n (\sqrt{\gamma^2(x-\beta t)^2 + y^2 + z^2})}}{4\pi \sqrt{\gamma^2(x-\beta t)^2 + y^2 + z^2}} \quad (46)$$

In the rest frame of the point source this reduces to the usual Yukawa form. The full solution is a sum over modes weighted by the f_n normalizations I_n^2 , see Eq. (35). There is a rapid rise in these normalizing factors with n which is due to the end point of the string being a delta function. Away from $N \rightarrow \infty$ one would expect the string to have some width and the expansion to truncate at some intermediate n . In any case this rise is not faster than the exponential fall off of the solutions so the physics away from the source is still dominated by the lightest modes. The Green’s function converges for all $|x| > 0$ due to the exponential factor in the Yukawa potential of each partial wave. The behaviour is dominated by the lighter modes at distances comparable to the Compton wavelength of the lightest mode. We interpret this Green’s function as the ‘dressing’ of an isolated quark by a cloud of mesons. Holography gives the relative amounts of each of the excited states in the cloud.

Radiation From String End Points

We now have a framework in which the emission of mesons can be modelled using the techniques of classical relativistic wave equations. The retarded Green’s function is straightforwardly integrated over the past worldline of an accelerating endpoint to give eg. for a particle moving in the x -direction (the u variable is as defined in the preceding section)

$$\langle J^0(x^\mu) \rangle_n = \frac{2(-1)^n I_n^2 q}{4\pi} \left[\frac{1}{t-t'(\sigma=0) - \frac{dx'}{dt'}(x-x'(\sigma=0))} + \int_0^\infty du \frac{J_1(u)}{t-t' - \frac{dx'}{dt'}(x-x')} \right] \quad (47)$$

We will again plot the baryon number density which is holographically encoded by the sum over the J_n^0 . It may be noted that the plots we obtain give the superposition of radiated baryon density and the static baryon density associated with the probe quark. An elementary prescription is available for computing the reaction force on the probe quark due to the radiation (by differencing the advanced and retarded potentials) but this is not what we are interested in here (it involves a negative counting of the non-causal advanced potential and so would not produce a plot resembling meson *emission*). In holographic scenarios (large N) the force exerted on the quark by the dynamics of the colour flux tube far exceeds the reaction force from meson emission anyway. In the case of an *instantaneous* acceleration it is possible to subtract the appropriate static and boosted solutions inside and outside of the particle’s light cone but we do not apply this here.

Massless Meson Limit

In the strict $\lambda \rightarrow \infty$ limit the meson masses are very small relative to the string mass (see (33)). At least for the lightest members of the tower, it is therefore interesting to compute the radiation into a massless gauge field on the D7. For this case $\sigma = \frac{1}{2}(-(t-t')^2 + (x-x'(t'))^2)$. The first term in (47) then gives

$$\begin{aligned} \langle J^0(x^\nu) \rangle_n &= \frac{2(-1)^n I_n^2 q}{4\pi} \int_{-\infty}^t dt' \delta(\sigma) \\ &= \frac{2(-1)^n I_n^2 q}{4\pi} \int \frac{d\sigma \delta(\sigma)}{((t'-t) + (x'-x) \frac{dx'}{dt'})} \\ &= \frac{2(-1)^n I_n^2}{4\pi} \frac{1}{t-t'(\sigma=0) - \dot{x}_0(x-x'(\sigma=0))} \end{aligned} \quad (48)$$

This is straightforward to evaluate for acceleration kicks such as those we found for the string end points in Figure

7 above. For example the static end point is accelerated quickly to a constant speed. As an example form for the function $x'(t')$ that describes a stationary particle accelerating to a final speed a we take

$$x'(t') = \frac{ab}{\pi} + at' \left(\frac{1}{2} + \frac{1}{\pi} \tan^{-1} \left(\frac{t'}{b} \right) \right) \quad (49)$$

b here controls the time interval over which the acceleration occurs - we plot some sample trajectories in Figure 8.

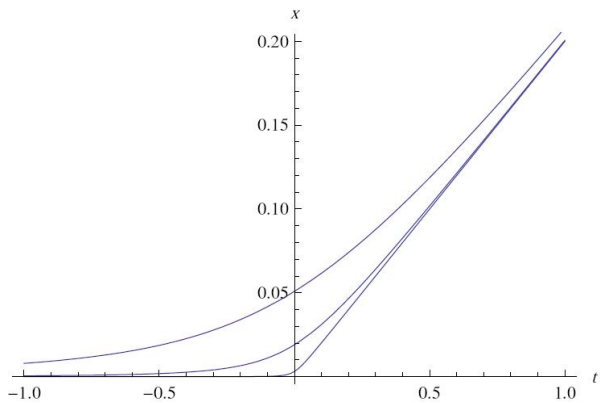


Figure 8: Plots of the function $x'(t')$ in (49) used to parameterize the motion of an accelerating point source. The parameter a controls the final speed and is set to $a = 0.2$ here. b controls the time scale of the acceleration and the plots show $b = 0.8$ (top), $b = 0.3$ (middle) and $b = 0.05$ (bottom).

It is a simple matter to plot the resulting wave induced. Emission is typically a spherical shell radiating from the point of acceleration - there is an $SO(2)$ symmetry in the y, z coordinates so we shall plot the intensity of the wave in the x, y plane at $z = 0$. Examples of the gauge field produced are shown in Figure 9. The radiative piece is visible along with the ‘hill’ of the boosted static potential. A clear, narrow emission wave is observable. For larger values of the final speed a the forward emission is typically enhanced relative to the backwards emission, and the overall emission is greater. For smaller acceleration times (smaller b) the wave front simply becomes narrower. For the accelerations of the string end points in Figure 7 we expect precisely such emission of the lower mass members of the mesonic tower.

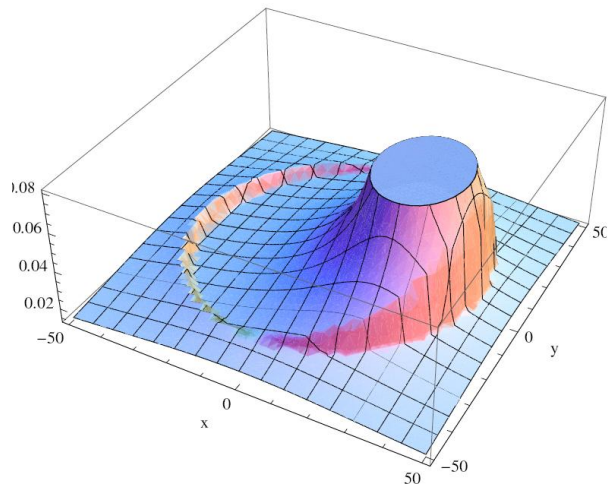
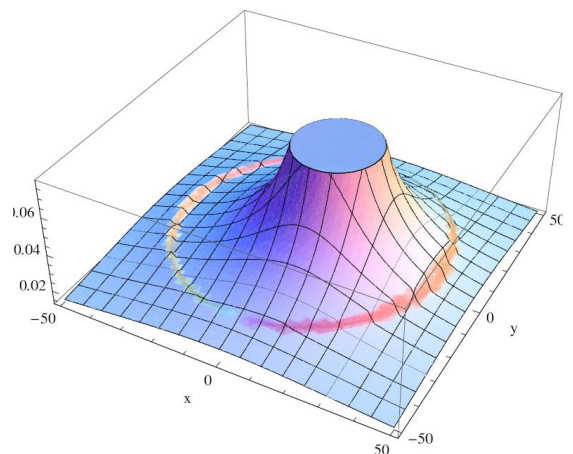


Figure 9: The radiation of light mesons by a quark given an impulse in the positive x -direction, shown in the $z = 0$ plane. The plot shows the density of the emitted (radiative part of field) and bound (boosted static part) mesons. The top plot is for a terminal velocity of $0.2c$ and below is $0.6c$ (in both plots the parameter $b = 0.2$).

Massive Meson Limit

For members of the meson tower with masses close to the quark mass (very high n at large 'tHooft coupling) we must compute the non-singular term in (47) which involves numerical integration of the Bessel function. In Figures 10 and 11 we show the effect of increased meson mass on the radiated mesons (the meson mass should be compared to the inverse time over which the string end point is accelerated). As the meson mass is increased we find emission of the more massive states are suppressed.

In the massive case the waves are dispersive and produce an interesting pattern which is not just a wave localized on the light-front. The ‘wavy’ emission of meson density

can be considered to be arising from quantum-mechanical interference effects.

In principle we could sum over the emission of all of the meson states. At large 'tHooft coupling though there are many states lighter than the quark mass so the result would be unilluminating. The precise form of the meson masses and the coefficients I_n^2 are also model dependent. However, we believe that the computations we have made show how in principle the radiation could be computed and give a good understanding of the generic features of that meson radiation.

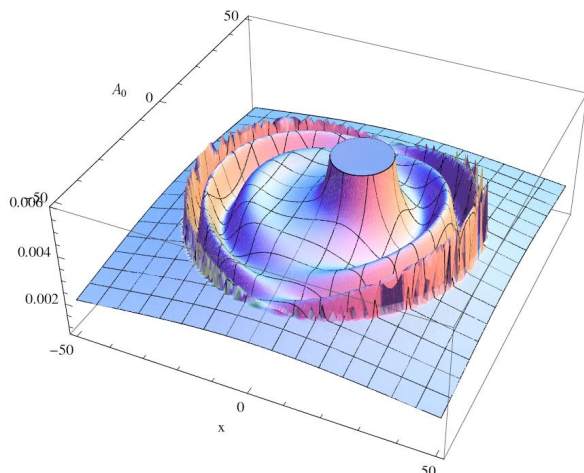


Figure 11: Emission of massive vector mesons ($m = \frac{1}{2}$). The parameters $a = b = 0.2$.

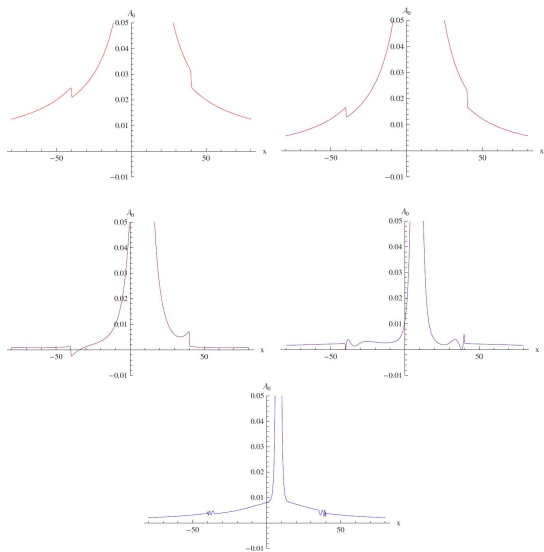


Figure 10: The radiation of massive mesons by a quark given an impulse in the positive x -direction, plotted along the x -axis. The plot shows the density of the emitted mesons. The meson masses increase through the plots as $0, 10^{-2}, 10^{-1}, \frac{1}{3}, 1$. Note the background static field peak becomes narrower as the mass is increased.

LESSONS FOR QCD

We have explored how a hadronization event happens in a gauge theory that has the degrees of freedom of $\mathcal{N} = 4$ super Yang-Mills in the UV but a deformation that leads to a back reacted hard wall and confinement in the IR. This theory, of course, is not QCD but the generic picture that emerges may have some lessons for the construction of a phenomenological model of hadronization in QCD.

In particular we have suggested a picture in which the initial quark anti-quark pair separate, growing a string between them that dips into a holographic radial direction. Initially the string's energy represents a $1/r$ potential between the quarks reminiscent of the asymptotically free regime of QCD. In actuality the $\mathcal{N} = 4$ theory is strongly coupled - one should ignore any radiation from this string (such as open string (glueball) radiation in the bulk) that would be present in the AdS/CFT Correspondence since that would be the wrong physics for QCD. The string then encounters a hard wall in the geometry and spreads out along it forming a traditional QCD-like string with energy growing with its length. We have proposed that this string will break quickly once there is sufficient energy in it to pair create a quark pair, breaking the string. The two sub-strings then separate, radiating energy through their end points as rho mesons. We expect the majority of the hadronization particle production to come from this radiation rather than repeated string breakings.

It is interesting to compare this picture to that of the Lund string model [41] which is one of the leading descriptions of hadronization used in accelerator Monte Carlos. The Lund model is based on the 1980s picture of the link between QCD and string theory. The strings

between quarks live in the 3+1d of QCD. The model assumes that a very long string forms between the quark anti-quark pair which then sequentially fragments with the fragments being assigned as various hadronic states. It's possible to morph our picture into the Lund one by assuming that the D7 brane in Figure 2 lies very close to the hard wall - the fifth dimension then plays little role and the string almost lies in the same plane as the end points move. How long the string grows and how many times it then breaks are not things we have computed so we can not dispute the Lund model. The striking difference though between the models is that significant rho meson production occurs at the end points of the string moving in AdS, removing the need for repeated breakings of the initial string. Of course the differences in the AdS picture may be an artefact of a large N expansion and not relevant to true QCD, but equally $N = 3$ is believed to not be so far from $N \rightarrow \infty$.

In theories close to the $\mathcal{N} = 4$ theory the rho mesons are special, in that they are associated with operators whose dimensions are protected from renormalization. This means they are present as supergravity modes in the DBI action of the D7 brane - other quark bound states would be represented by stringy states also tied to the D7 world volume. In QCD we would not expect a separation in character between these modes and all hadronic species should be produced at the end point governed by the same end point motion.

The idea of separating, radiating string fragments is reminiscent of another reasonably successful model of hadronization. Thermal models [42] have been proposed that treat the event as separating fireballs radiating hadrons in thermal equilibrium. Some discussion of how that thermal spectrum can emerge from a gauge theory event with many final states even at zero temperature can be found in [43, 44] - it seems likely that the core idea is just that the energy of hadronization is freely available to all modes. A very toy model of holographic hadronization was presented, based on these ideas, in [45] - there an equal lump of energy was dumped into the 5d holographic fields associated with each set of QCD bound states with a Gaussian profile in the radial direction. The model seemed to reproduce the data reasonably well too. [46] Here one can associate that lump of energy to the wave of gauge field emitted by the string end point as shown in Figures 9-11.

It's therefore interesting that our holographic model seems to include aspects of both the Lund string model and thermal models of hadronization. We hope that insights from AdS will lead to phenomenologically more successful models of hadronization in QCD in the future.

Acknowledgements: JF and ET would like to thank STFC for their studentship funding. NE is funded by an STFC rolling grant and is grateful to Marija Zamaklar and Kasper Peeters for discussions. KJ would like to thank Andreas Karch for many fruitful conversations. KJ was supported in part by the U.S. Department of Energy under Grant No. DE-FG02-96ER40956.

-
- [1] J. M. Maldacena, Adv. Theor. Math. Phys. **2**, 231 (1998) Int. J. Theor. Phys. **38**, 1113 (1999) [arXiv:hep-th/9711200].
 - [2] E. Witten, Adv. Theor. Math. Phys. **2** (1998) 253 [arXiv:hep-th/9802150].
 - [3] E. Witten, Adv. Theor. Math. Phys. **2** (1998) 505 [arXiv:hep-th/9803131].
 - [4] S. S. Gubser, I. R. Klebanov and A. M. Polyakov, Phys. Lett. B **428** (1998) 105 [arXiv:hep-th/9802109].
 - [5] M. Grana and J. Polchinski, Phys. Rev. **D65** (2002) 126005, [arXiv: hep-th/0106014].
 - [6] M. Bertolini, P. Di Vecchia, M. Frau, A. Lerda and R. Marotta, Nucl. Phys. B **621**, 157 (2002) [arXiv:hep-th/0107057].
 - [7] I. Kirsch and D. Vaman, Phys. Rev. **D72** (2005) 026007, [arXiv: hep-th/0505164]
 - [8] A. Karch and E. Katz, JHEP **0206**, 043 (2002) [arXiv:hep-th/0205236].
 - [9] M. Kruczenski, D. Mateos, R. C. Myers and D. J. Winters, JHEP **0307** 049, 2003 [arXiv:hep-th/0304032].
 - [10] J. Babington, J. Erdmenger, N. J. Evans, Z. Guralnik and I. Kirsch, Phys. Rev. D **69** (2004) 066007 [arXiv:hep-th/0306018].
 - [11] K. Ghoroku and M. Yahiro, Phys. Lett. B **604** (2004) 235 [arXiv:hep-th/0408040].
 - [12] J. Erdmenger, N. Evans, I. Kirsch and E. Threlfall, arXiv:0711.4467 [hep-th].
 - [13] S. D. Ellis, J. Huston, K. Hatakeyama and P. Loch, Prog. Part. Nucl. Phys **100** (2008) 484 [arXiv:0712.2447 [hep-ph]].
 - [14] L. F. Alday and J. Maldacena, JHEP **0711** (2007) 068 [arXiv:0710.1060 [hep-th]].
 - [15] Y. Hatta, E. Iancu and A. H. Mueller, JHEP **0805** (2008) 037 [arXiv:0803.2481 [hep-th]].
 - [16] P. M. Chesler, K. Jensen and A. Karch, Phys. Rev. D **79** (2009) 025021 [arXiv:0804.3110 [hep-th]].
 - [17] J. M. Maldacena, Phys. Rev. Lett. **80** (1998) 4859 [arXiv:hep-th/9803002].
 - [18] S. J. Rey and J. T. Yee, Eur. Phys. J. C **22** (2001) 379 [arXiv:hep-th/9803001].
 - [19] C. P. Herzog, A. Karch, P. Kovtun, C. Kozcaz and L. G. Yaffe, JHEP **0607** (2006) 013 [arXiv:hep-th/0605158].
 - [20] S. S. Gubser, Phys. Rev. D **74** (2006) 126005 [arXiv:hep-th/0605182].
 - [21] L. Girardello, M. Petrini, M. Porrati and A. Zaffaroni, JHEP **9812** (1998) 022 [arXiv:hep-th/9810126].
 - [22] K. Pilch and N. P. Warner, Nucl. Phys. B **594** (2001) 209 [arXiv:hep-th/0004063].
 - [23] L. Girardello, M. Petrini, M. Porrati and A. Zaffaroni, Nucl. Phys. B **569** (2000) 451 [arXiv:hep-th/9909047].

- [24] K. Pilch and N. P. Warner, *Adv. Theor. Math. Phys.* **4** (2002) 627 [arXiv:hep-th/0006066].
- [25] J. Polchinski and M. J. Strassler, arXiv:hep-th/0003136.
- [26] J. Babington, D. E. Crooks and N. J. Evans, *Phys. Rev. D* **67** (2003) 066007 [arXiv:hep-th/0210068].
- [27] A. Kehagias and K. Sfetsos, *Phys. Lett. B* **454** (1999) 270 [arXiv:hep-th/9902125].
- [28] S. S. Gubser, arXiv:hep-th/9902155.
- [29] N. R. Constable and R. C. Myers, *JHEP* **9911** (1999) 020 [arXiv:hep-th/9905081].
- [30] J. Polchinski and M. J. Strassler, *Phys. Rev. Lett.* **88** (2002) 031601 [arXiv:hep-th/0109174].
- [31] J. Erlich, E. Katz, D. T. Son and M. A. Stephanov, *Phys. Rev. Lett.* **95** (2005) 261602 [arXiv:hep-ph/0501128].
- [32] L. Da Rold and A. Pomarol, *Nucl. Phys. B* **721** (2005) 79 [arXiv:hep-ph/0501218].
- [33] I. H. Brevik, K. Ghoroku and A. Nakamura, *Int. J. Mod. Phys. D* **15** (2006) 57 [arXiv:hep-th/0505057].
- [34] J. Dai and J. Polchinski, *Phys. Lett. B* **220** (1989) 387.
- [35] F. Bigazzi and A. L. Cotrone, *JHEP* **0611** (2006) 066 [arXiv:hep-th/0606059].
- [36] A. L. Cotrone, L. Martucci and W. Troost, *Phys. Rev. Lett.* **96** (2006) 141601 [arXiv:hep-th/0511045].
- [37] K. Peeters, J. Sonnenschein and M. Zamaklar, *JHEP* **0602** (2006) 009 [arXiv:hep-th/0511044].
- [38] N. Evans and E. Threlfall, *Phys. Rev. D* **78** (2008) 105020 [arXiv:0805.0956 [hep-th]].
- [39] K. Peeters, J. Plefka and M. Zamaklar, *JHEP* **0411** (2004) 054 [arXiv:hep-th/0410275].
- [40] E. Poisson, *Living Rev. Rel.* **7** (2004) 6 [arXiv:gr-qc/0306052].
- [41] B. Andersson, G. Gustafson, G. Ingelman and T. Sjostrand, *Phys. Rept.* **97** (1983) 31.
- [42] F. Becattini, *Z. Phys. C* **69** (1996) 485.
- [43] J. Hormuzdiar, S. D. H. Hsu and G. Mahlon, *Int. J. Mod. Phys. E* **12** (2003) 649 [arXiv:nucl-th/0001044].
- [44] Y. Hatta and T. Matsuo, *Phys. Rev. Lett.* **102** (2009) 062001 [arXiv:0807.0098 [hep-ph]].
- [45] N. Evans and A. Tedder, *Phys. Rev. Lett.* **100** (2008) 162003 [arXiv:0711.0300 [hep-ph]].
- [46] Note to compare to data there is the need to impose an elaborate decay chain between the initially produced particles and the finally observed particles so the number of species for which there is data is much less than the total number of species in the initial yield which may hide many evils.